Published in final edited form as:
Alcohol Clin Exp Res. 2013 December ; 37(12): 2074–2085. doi:10.1111/acer.12204.

Long-term modulation of A-type K^+ conductances in hippocampal CA1 interneurons in rats after chronic intermittent ethanol exposure during adolescence or adulthood

Qiang Li[1,2,3], **Rebekah L. Fleming**[1,2], **Shawn K. Acheson**[1,2], **Roger D. Madison**[1,3], **Scott D. Moore**[1,2], **Mary-Louise Risher**[1,2], **Wilkie A. Wilson**[1,2], and **H.S. Swarztwelder**[1,2]

[1]Durham VA Medical Center, Departments of Duke University Medical Center, Durham, North Carolina, USA 27705

[2]Medical Psychiatry, Duke University Medical Center, Durham, North Carolina, USA 27705

[3]Neurosugery, Duke University Medical Center, Durham, North Carolina, USA 27705

Abstract

Background—Chronic alcohol use, especially exposure to alcohol during adolescence or young adulthood, is closely associated with cognitive deficits that may persist into adulthood. Therefore, it is essential to identify possible neuronal mechanisms underlying the observed deficits in learning and memory. Hippocampal interneurons play a pivotal role in regulating hippocampus-dependent learning and memory by exerting strong inhibition on excitatory pyramidal cells. The function of these interneurons is regulated not only by synaptic inputs from other types of neurons, but is also precisely governed by their own intrinsic membrane ionic conductances. The voltage-gated A-type potassium channel (I_A) regulates the intrinsic membrane properties of neurons, and disruption of I_A is responsible for many neuropathological processes including learning and memory deficits. Thus, it represents a previously unexplored cellular mechanism whereby chronic ethanol may alter hippocampal memory-related functioning.

Methods—Using whole cell electrophysiological recording methods we investigated the enduring effects of chronic intermittent ethanol exposure (CIE) during adolescence or adulthood on I_A in rat CA1 interneurons.

Results—We found that the mean peak amplitude of I_A was significantly reduced after CIE in either adolescence or adulthood, but I_A density was attenuated after CIE in adolescence but not after CIE in adulthood. In addition, the voltage dependent steady-state activation and inactivation of I_A were altered in interneurons after CIE.

Conclusions—These findings suggest that CIE can cause long-term changes in I_A channels in interneurons and thus may alter their inhibitory influences on memory-related local hippocampal circuits, which could be, in turn, responsible for learning and memory impairments observed after chronic ethanol exposure.

Send correspondence to: Dr. H.S. Swartzwelder Department of Psychiatry Duke University Medical Center and Durham VA Medical Center Room 24, Building 16, VAMC 508 Fulton Street, Durham NC 27705 Tel: (919) 971-0964 HSS@duke.edu.

Keywords

I_A channels; interneurons; hippocampus; chronic intermittent ethanol exposure (CIE); adolescence; development

Introduction

Most people in the U.S. begin to use ethanol during adolescence, during which there is a high prevalence of heavy intermittent drinking (NIAAA 2000). The brain undergoes substantive changes in structure and function during adolescence and responds in distinctive ways to acute ethanol (Dahl 2004; Monti et al. 2005), yet little is known about the enduring consequences of adolescent ethanol exposure on neuronal function in adulthood.

Hippocampal interneurons located within the stratum-radiatum and stratum-lacunosummoleculare of area CA1 (SR-SLM interneurons) produce feed-forward inhibition of CA1 pyramidal neurons (Empson and Heinemann, 1995). They form inhibitory synapses on the distal portions of apical dendrites of pyramidal cells (Lacaille and Schwartzkroin, 1988) and thereby modulate the incoming excitatory glutamatergic drive that induces long-term potentiation (LTP). This inhibition also controls temporal summation of excitatory inputs onto CA1 pyramidal cells (Pouille and Scanziani, 2001; 2004) and is activated at the peak of theta oscillations (Tukker et al, 2007), which are related to learning (Elfant et al 2008, Freund and Buzsaki 1996, Freund and Gulyas, 1997, Vida et al. 1998). Thus, the effects of ethanol on interneuron firing may underlie its inhibition of hippocampus-dependent learning. That these interneurons are more sensitive to ethanol during adolescence than adulthood (Yan et al 2009) is consistent with observations that EtOH disrupts spatial learning more potently in adolescent animals than in adults (Markweise et al, 1998).

Chronic ethanol alters neuronal function and synaptic transmission (Littleton 1998; Gonzalez 1998), possibly due to changes in ionic conductances, though the effects of chronic ethanol exposure on neuronal ionic conductances remain poorly understood. Despite their abundant expression, the effects of chronic ethanol on I_A channels in hippocampal interneurons are virtually unknown (Martina et al 1998; Lien et al, 2002, Lien and Jonas 2003; Bourdeau et al., 2007; 2011). Given that I_A plays a critical role in regulating neuronal firing (Kang et al, 2000, Morin et al, 2010, Carrsquillo et al, 2012), neurotransmitter release (Cooper et al 1998) and responses to synaptic inputs (Hoffman et al 1997; Jerng et al, 2004), I_A channels may serve as a substrate through which ethanol exerts its acute and long-lasting actions on neuronal function.

I_A channels participate in acute and chronic ethanol effects on neuronal function. At high concentrations, ethanol inhibits I_A in invertebrate neurons (Treistman and Wilson, 1987; Alekseev et al 1997), but it is not clear whether acute concentrations of ethanol in a range consistent with human intoxication alter I_A. Despite a paucity of evidence related to the acute effects of ethanol on I_A, chronic ethanol exposure has been shown to affect it. For example, chronic ethanol exposure during the early postnatal period in rats down-regulates the expression of I_A channel subunit proteins Kv3.2 and 3.4 in the neocortex (Tavian et al

2011), and chronic ethanol exposure during adulthood increased the amplitude of I_A in nucleus accumbens medium spiny neurons (Marty and Spigelman, 2012). Thus, I_A is an important mediator of neuronal function that is sensitive to the long-term effects of chronic ethanol exposure. The present experiments were designed to assess the enduring effects of chronic ethanol exposure, during adolescence or adulthood, on I_A in SR-SLM interneurons.

Materials and Methods

Male Sprague Dawley rats (Charles River, Raleigh, NC) were double-housed with *ad libitum* access to food and water, acclimatized for 5-6 days in the VA Medical Center vivarium on a reversed 12:12-hr light:dark cycle (lights off at 9 a.m.), and handled daily for four days prior to the initiation of chronic intermittent treatment with EtOH or saline. Postnatal day (PD) 30 (adolescent) and PD 70 (adult) rats were treated with 10 doses of 5g/kg ethanol (35% w/v in 0.9% saline) or the saline vehicle by gavage using a two-days-on, two-days-off schedule, for 20 days (during the animals' dark phase) followed by a 20-day washout period prior to the initiation of electrophysiological experiments.

Rats were deeply anaesthetized with isoflurane and transcardially perfused with a chilled oxygenated solution containing (in mM) N-methyl-D-glucamine (NMDG) 115, KCL 3.3, $NaHCO_3$ 25, $NaH_2PO_4H_2O$ 1.23, $CaCl_2$ 0.2,$MgSO_4$ 12, myo-insitol 3, Na pyruvate 2, Na ascorbate 0.4 and glucose 10. The rat was then decapitated and the brain quickly removed and placed in the same solution. Transverse hippocampal slices (300-μm) were cut with a moving blade microtome and placed in oxygenated artificial cerebrospinal fluid (aCSF) containing (in mM): NaCl 120, KCl 3.3, $NaHCO_3$ 25, $NaH_2PO_4H_2O$ 1.23, $CaCl_2$ 1.8, $MgSO_4$ 1.2, and glucose 10 at 35°C for 60 minutes. The slices were then maintained at room temperature until recording.

The recording chamber was perfused (~3 mL/min) with oxygenated aCSF at 35°C. SRSLM interneurons were identified under a Zeiss microscope equipped with a 40× water immersion objective and an enhanced differential interference contrast video system. Recording pipettes with resistance of 4–8 MΩ were pulled from borosilicate glass capillaries (1.5mm OD) using a P97 electrode puller (Sutter Instruments). The pipette solution contained (in mM); K- gluconate 120, KCL 10, $MgCl_2$ 5, $CaCL_2$ 0.06, EGTA 0.6, Mg ATP 2, Tri-GTP 0.3, phosphocreatine 10, creatine-phosphokinase 50, and HEPES 10. The pH was adjusted to 7.4 with KOH and osmolarity was 290mOsm. Recordings were performed at 35°C.

I_A was recorded in voltage clamp mode using an Axopatch 200B amplifier (Molecular Devices, LLC. Sunnyvale, CA). Signals were filtered at 5kHz, digitized at 10kHz, and acquired by a computer using a Digidata 1440 analog-to-digital converter (Molecular Devices, Sunnyvale, CA). Leak and capacitive currents were subtracted online using P/4 procedures. To record I_A the following reagents were added to the external solution: 20mM tetraethylammonium (TEA), 1.0μM tetrodotoxin (TTX), and 0.3mM cadmium chloride. Excitatory and inhibitory synaptic transmission was also blocked using DNQX (10μM), AP5 (50μM), and picrotoxin (75μM). Interneurons were voltage clamped at -70mV. To isolate I_A, cells were hyperpolarized to -110mV for 100ms to elicit maximal conductance prior to being depolarized to +40mV in 10mV increments for 400ms. In the second protocol, cells were

pre-pulsed to -10mV for 100ms followed by depolarization to +40mV in 10mV increments for 400ms. The outward currents elicited by the second protocol were digitally subtracted from the first to yield I_A (Figure 1). Steady-state activation curves were determined using data collected from the isolated I_A. Steady-state inactivation curves were constructed using the following protocol: 100-ms pre-pulses of varying potentials (–120 to –0mV, 10mV steps) followed by a 400-ms step at +20mV. To determine I_A recovery kinetics following inactivation, a double-pulse protocol consisting of varied test-pulse intervals was used. The membrane capacitance obtained using the Clampex seal test function was used as the value for whole-cell capacitance. Series resistance was monitored throughout experiments and neurons with resistance changes greater than 15% were discarded.

The density of I_A was calculated by dividing the peak current amplitude at each test voltage by the membrane capacitance. To obtain steady-state activation curves, chord conductance (G) was calculated from the peak currents using the following equation: G=I/(Vm-Vk), where *I* was the current amplitude, *Vm* was the command potential, and Vk was the reversal potential (-98mV in our recording conditions). I_A conductance was then normalized to the maximal conductance and plotted as a function of the command potential. After steady-state activation and inactivation curves were established, they were fitted with functions based on the Boltzmann equation: $f = A2+(A1-A2)/\{1+\exp[(Vm-V_{1/2})/k]\}$, where A1 and A2 are the initial and final values, Vm is the membrane potential, $V_{1/2}$ is the potential at which the value of the Boltzmann function is 0.5, and k is the slope factor.

Experimenters were blind to the treatment condition of animals until after data analyses were complete. Data were analyzed using ClampFit-10 (Molecular Devices, Sunnyvale, CA), Origin-8.0 and Microsoft Excel, and are presented as mean ±SEM. Student's *t*-tests were used to infer significant differences between two group means. Alternatively, Welch's *t*-test was used where homogeneity of variance could not be assumed. In all instances, alpha was set at $p < 0.05$.

Results

Interneurons were readily visualized under infrared DIC (Fig-1F). I_A was isolated by taking advantage of the inactivation kinetics of the channel and applying two different voltage pulse protocols, as illustrated in Fig-1A-B. An interneuron from a slice from an adolescent rat pretreated with saline was voltage clamped at -70mV and was first hyperpolarized to -110mV for 100ms and then depolarized for 400ms. The depolarization pulses were stepped from -100mV to +40mV in 10mV increments. Pre-pulse of hyperpolarization at -110mV removed I_A channel inactivation and enabled subsequent maximum activation. The voltage protocols, shown as an inset in Fig.1A, evoked rapidly activating outward currents. The same cell was also depolarized by the same voltage steps preceded by a depolarizing pre-pulse of -10mV for 100ms. Under those conditions, slowly inactivating currents became evident. The voltage responses are illustrated in Fig. 1B. Digital subtraction of the voltage responses elicited by the pre-pulse hyperpolarization, from those elicited by the pre-pulse of depolarization, yielded a transient fast activating and inactivating outward I_A. The subtracted voltage traces under each of the membrane test potentials are shown in Fig-1C. I_A exhibited strongly voltage dependent activation, which became more apparent after plotting

the normalized I_A conductance as a function of the testing potentials, as shown in Fig. 1D. Additionally, the plot for this neuron was fit best with a single Boltzmann function to obtain a half maximal activation potential of -18mV and a slope of factor 11mV (Fig. 1E).

Chronic intermittent ethanol exposure reduced peak I_A amplitude

Two typical examples of I_A recorded from animals exposed to saline (left panel) or CIE (right panel) during adolescence are shown in Fig. 2A. The peak amplitude of I_A was markedly smaller in the interneuron from the ethanol-pretreated animal at more positive test potentials.

For example, at +40mV, the peak amplitude was 5.3nA in this interneuron recorded from the rat pretreated with saline during adolescence but was only 2.2nA in the interneuron from the animal pretreated with ethanol during adolescence.

I_A was recorded from 13 interneurons from rats (n=4) exposed to ethanol during adolescence and 10 interneurons from rats (n=4) exposed to saline during adolescence. The mean peak amplitudes of I_A obtained from both groups were plotted as a function of the membrane test potentials and are shown in the left panel of the Fig. 2B. In interneurons from CIE rats the mean peak amplitude of I_A was significantly reduced compared to those from saline-pretreated rats. The average amplitude of I_A elicited at +40mV in slices from saline pretreated rats was significantly larger than those from CIE pretreated rats ($t(21) = 2.55$, $p=0.0186$).

Figure 2C shows two representative I_A traces isolated from interneurons from animals pre-exposed to saline (left panel) or ethanol (right panel) during adulthood. Similar to the findings observed in cells from rats treated during adolescence, CIE pre-treatment in adulthood reduced the peak amplitude of I_A. At 40mV, peak amplitude was 3.2nA in the interneuron from the saline pre-treated rat, but was only 1.8nA in the interneuron from the ethanol pre-treated rat. The mean peak amplitudes of I_A obtained from both groups treated in adulthood were plotted as a function of the testing potentials and are shown in the left panel of the Fig-2D. I_A was recorded from nine interneurons from rats (n=4) exposed to ethanol during adulthood and 15 interneurons from rats (n=4) exposed to saline during adulthood. On average, the peak amplitude of I_A was significantly reduced in cells from rats that received CIE during adulthood (n=4) compared to controls (n=4). Average amplitude of I_A elicited at +40 mV in CIE rats is significantly smaller than in control rats ($t(22) = 1.72$, $p=0.0497$).

Thus, CIE during either adolescence or adulthood caused a significant reduction in the peak amplitude of I_A. However, we also found that, for both age groups, the capacitances of interneurons from CIE-treated rats were significantly lower than those from control rats (Adolescent group: CIE: 19.5 ± 1.25pF (n=13) vs. saline: 24.9 ± 0.96pF (n=10), $t(21)=4.2045$, $p=0.0039$. Adult group: CIE: 16.5 ± 2.06pF (n=15) vs. saline: 23.6 ± 1.72pF (n=9), $t(22) = 2.4997$, $p= 0.0203$). We next assessed if the reductions in I_A amplitude persisted after normalizing for changes in cell capacitance by calculating the current density of I_A. There was no overall effect of age on I_A density at +40mV ($F(1, 45) = 1.02$, $p = 0.32$). However, I_A density was significantly reduced in interneurons from animals pretreated with

CIE during adolescence (right panel of the Fig. 2B, Welch t-test, t(15.52)=1.83, p=0.0427), but not in those from animals pretreated with CIE during adulthood (right panel in Fig. 2D).

Effects of CIE on steady-state activation of I_A

We next assessed the effect of CIE on the voltage dependence of I_A by constructing steady-state activation curves. We normalized the conductance at each test potential to the conductance obtained at +40mV, averaged them for all interneurons in the same age and pretreatment group, and then plotted them as a function of the test potentials. For animals pretreated with ethanol or saline during adolescence, I_A became detectable around -40mV, with strong activation observed at more positive test potentials. The activation curve for each individual interneuron was fit with a single Boltzmann function to obtain the half-activation potential and the slope factor. CIE pretreatment during adolescence shifted the activation curve to the right compared to controls (Fig. 3A). The averaged results are illustrated in Fig. 3C (half-activation potentials) and 3D (slope factors). There was a significant change in the half-activation potential (CIE: 4.08± 2.86mV, n=10 and saline: -10.53± 5.06mV, n=9, t(17)= -2.5835. p=0.0193). There was no significant difference in the slope factors (CIE:14.25± 1.01mV and saline: 11.79± 0.70mV, t(17)=-1.9465, p=0.068), indicating that cells from animals that received CIE during adolescence had significantly higher half activation potentials than did those from their age-matched control animals. In cells from animals pretreated as adults, beginning at -40mV, the mean activation curve of I_A in cells from animals pretreated with ethanol during adulthood was slightly shifted to the left compared to that in cells from saline pretreated rats (Fig. 3B). However, CIE pretreatment during adulthood did not significantly alter either the half-activation potentials (Fig. 3C) (CIE: -12.69± 2.68mV, n=7 and saline: -5.31± 2.68mV, n=12, t(17)=1.89435, p=0.0753) nor the slope factors (Fig. 3D)(CIE: 12.67± 0.88mV and saline: 14.98± 1.20mV, t(17)=1.34466, p=0.1964). These results indicate that CIE during adolescence, but not during adulthood, alters steady-state activation of I_A.

Effects of CIE on steady-state inactivation of I_A

Figure 4A shows a typical example of I_A elicited by a voltage protocol (inset graph). A depolarizing test potential to +20mV for 400ms was applied following a pre-pulse potential during which the membrane potentials were stepped from -120mV to 0mV in 10mV increments. Peak I_A was normalized to the peak current elicited from the most hyperpolarized test potential and plotted as a function of the test potential. The voltage-dependent steady-state inactivation curves of I_A are shown in Fig. 4B for interneurons from animals pretreated during adolescence and in Fig. 4C for those from animals pretreated as adults. Overall, the steady-state I_A inactivation curves for cells from animals pretreated with CIE were shifted to the right relative to those from age-matched controls. Moreover, regardless of age and treatments, complete inactivation of I_A was evident at test potentials more depolarized than -20mV. The mean half-inactivation potentials were significantly shifted toward depolarized potentials in interneurons from animals pretreated with CIE compared to controls (Fig. 4D). In interneurons from animals pretreated with CIE during adolescence, the mean half-inactivation potential was -48.79± 2.91mV (n=9), and for those pretreated with saline it was -66.04± 2.05mV (n=10) (t(17)=4.91922, p=0.00012). Among cells from animals pretreated as adults, the mean half-activation potential was -57.39±

1.85mV for those pretreated with CIE (n=7), and -64.55± 2.69mV for those pretreated with saline (n= 11)(t(15)=-2.18749, p=0.04409). In contrast, the mean slope factors (Fig. 4E) were not affected by CIE pretreatment at either age (adolescent: 8.49 ± 0.69mV for saline and 8.27 ±1.04mV for CIE, t(17)=0.17851, p=0.86043; adult: 10.42± 0.96mV for saline and 7.97 ± 0.94mV for CIE, t(16)=1.7258, p=0.10364). When the activation and inactivation curves were plotted together as a function of test membrane potentials, the intersection of activation and inactive curves and window currents can be observe in Figs. 4F and 4G. In Fig. 4F, the interaction point of mean activation and inactivation curves was shifted from -43mV for rats pretreated with saline to -28mV for CIE rats. In the adult pre-treatment group the two curves cross at -39mV for saline rats and -34mV for CIE rats.

Effects of CIE on I_A recovery from inactivation

The activity of I_A also depends on the rate of recovery from inactivation. Given the fact that hippocampal interneurons can fire action potentials with a frequency as high as 100Hz, the rate of recovery from inactivation of I_A may also be sensitive to CIE. The time course of recovery from inactivation of I_A in an interneuron from an animal pretreated with saline during adolescence is shown in Fig. 5A. The two-pulse voltage protocol used to evoke I_A is also illustrated as an inset to Fig. 5A. The first pulse depolarized the membrane potential to +20mV from -70mV for 400ms and then the membrane potential was stepped to +20mV for 400ms again following a variable inter-pulse interval of 1 to 1000ms. The fraction of the maximum current evoked by the first pulse, in response to recovered current evoked by the second pulse, served as a measure of the time-dependent recovery of channel availability for the subsequent activation. As depicted in Fig. 5A, a progressive increase in the amplitude of I_A was observed. The amplitude of I_A obtained during the first 200ms is also shown at a faster time scale in the right panel. The normalized peak amplitudes of I_A were plotted as a function of the test potentials and are shown in Fig. 5B for rats pretreated during adolescence and 5C for rats pretreated as adults. The graphs illustrating the recovery from inactivation for the first 200ms are shown in the right panels of Figure 5B&C. The rates, or time constants (TC), of recovery were assessed by fitting the curves with a double exponential function for each of the interneurons. Pretreatment did not alter fast decay time constants in interneurons from CIE rats (Fig. 5D, Adolescent: t(17)= 0.713, p=0.48547, Adult: t(17)= -2.0388, p=0.05733). However, the mean slow decay time constant was significantly longer in cells from animals pretreated with CIE, compared to controls, independent of the age at which the pretreatment occurred (Fig. 5E, Adolescent: t(17)= -2.133, p=0.0479; Adult: t(17)= -2.604, p=0.01825).

Effects of CIE on the decay kinetics of I_A

We further investigated the decay of I_A by fitting the current traces obtained at +30mV with a double exponential function. As shown in Fig. 6A, the representative current trace that could be best fitted by a double exponential function is indicated by a dotted line, and two components, a fast and a slow TC, were obtained and averaged for comparison. CIE did not alter the fast TCs of cells from animals pretreated during adolescence or adulthood (Fig. 6B, Adolescent: t(23)= -0.286, p=0.7743; Adult: t(22)=0.669,p=0.51054). The fast TCs appeared larger in cells from animals treated as adults, but there was not a significant overall effect of age on TC (F(1, 45) = 2.87, p = 0.10). In contrast, CIE increased the slow decay time in cells

from animals pretreated during adolescence and decreased slow decay time in cells from animals pretreated during adulthood (Figure 6C). The mean slow TC obtained from rats pretreated with CIE during adolescence, at the test potential of +30mV, was significantly prolonged compared to controls (TCs: for saline, 37.82 ± 9.45ms, n=13, CIE: 95.58 ± 29.2ms, n=12, t(23)=-1.95, p=0.0317), whereas the mean slow TCs obtained from rats pretreated with CIE as adults, at the same test potential, was significantly shortened compared to controls (saline, 75.11 ± 20.19ms, n=15, CIE: 28.24 ± 6.8ms ,n=9, t(22)=1.75, p=0.0470).

Discussion

CIE pre-treatment caused a significant and long lasting reduction in the peak amplitude of I_A currents in CA1 interneurons independent of whether the CIE occurred in adolescence or adulthood. However, CIE pre-treatment during adolescence caused a more profound reduction of subsequent I_A current density than did CIE pre-treatment in adulthood. Furthermore, interneurons from animals that received CIE during adolescence had significantly higher half activation potentials than did those from their age-matched controls, whereas no such effect was observed when CIE occurred during adulthood. CIE also produced a long-term increase in I_A slow decay time when presented in adolescence, and a long-term decrease in slow decay time when presented in adulthood. The half-activation data suggest that after CIE in adolescence, but not adulthood, I_A conductance is enduringly altered such that a greater state of depolarization is required for its activation. This would be expected to result in higher interneuron firing rates and could be of mechanistic significance for understanding the long-term effects of ethanol exposure during adolescence on learning and memory. In addition, this is the first demonstration that I_A in CA1 interneurons is enduringly altered by chronic ethanol exposure, suggesting that the conductance of this current represents a fundamental neurophysiological mechanism underlying the chronic effects of ethanol on CNS function.

I_A channels are expressed in many types of neurons (Coetzee et al, 1999; Binbaum et al, 2004; Maffie and Rudy, 2008) and play a critical role in regulating neuronal function. Since I_A channels possess features such as fast activation, inactivation, rapid recovery, and voltage-gated sub-threshold activation, they regulate a number of neuronal functions critical for controlling neuronal excitability and firing frequency (Lien and Jonas, 2003; Liss et al. 2001; Khaliq and Bean. 2008, Johnston et al 2010) as well as synaptic plasticity (Kole et al 2007; Jung et al 2008; Kim and Hoffman 2008). In addition, the activity of I_A channels is sensitive to various neuromodulators (An et al 2000; Cai et al 2007). Whether ethanol can modulate I_A channels remains controversial, and is unknown for I_A channels expressed in CA1 interneurons. Studies using Aplysia neurons indicated that I_A amplitude was increased and inactivation was decreased by acute ethanol, but only at very high concentrations (200 to 400mM)(Treistman and Wilson, 1987). Alekseev et al. also (1997) reported that, in Lymnaea neurons, a very high concentration of ethanol (830mM) suppressed I_A. However, there are very few studies of ethanol effects on I_A in mammalian neurons. One such report has shown that acute ethanol at a low dose inhibits, but at a high dose enhances, I_A currents in cultured cerebellar granule neurons from rats (Lefebvre et al, 2009). The present findings demonstrate, for the first time, that in-vivo CIE results in a long-lasting change in the gating

properties of I_A channels expressed in CA1 interneurons, thus suggesting a new mechanism underlying the enduring effects of chronic ethanol exposure. In addition, our results are consistent with a recent report in which the level of expression of Kv3.2 and 3.4, a family of subunit proteins encoding I_A channels, was significantly down-regulated in cortical neurons from rats exposed to ethanol chronically during the first week after birth (Tavian et al 2011). Thus it may be that the effects of chronic ethanol on neuronal excitability are modulated to a large degree, and in a wide number of neuronal types, by its effects on the protein subunits that constitute and maintain I_A channels.

In a recent report, Marty and Spigelman (2012) found that CIE treatment in adult rats resulted in an increase in the amplitude of I_A in the medium spiny neurons in the nucleus accumbens, whereas we found a long-term down regulation of I_A in the hippocampus. This divergence suggests that the effect of CIE on I_A may be cell-type-specific. It may also reflect differences in the location and functions of the neurons studied, and, more importantly, the diversified molecular components encoding the I_A channels in these neurons (Tkatch et al 2000).

CIE decreased cell capacitance in both age groups, but I_A density was only significantly reduced in neurons from animals pre-treated with CIE during adolescence, not in those who were pre-treated in adulthood. However, peak I_A amplitude was reduced by CIE pre-treatment in either adolescence or adulthood. This suggests that mechanisms other than those associated with capacitance may drive the effects of chronic ethanol exposure during adolescence, compared to adulthood. It is not clear why CIE reduced subsequent I_A density when applied in adolescence but not in adulthood, but it is possible that neurodevelopmental changes during adolescence, combined with CIE, may alter the expression profile of I_A subunits.

The present findings may also help explain the functional roles of I_A in CA1 interneurons in the hippocampus, especially their roles in LTP formation. Mice with genetic deletion of the Kv4.2 subunit exhibit deficits in hippocampal-dependent learning (Lugo et al, 2012), indicating that an ablation of genes mediating I_A channels disrupts learning. CIE during adolescence in rats has been shown to impair learning in adulthood (Sircar and Sircar, 2005), and to render animals more susceptible to the memory impairing effects of acute ethanol (White et al, 2000). Thus, down regulation of I_A currents in SR-SLM interneurons would be expected to lead to increased firing of those cells, and more downstream inhibition on the distal dendrites of CA1 pyramidal cells (Lacaille and Schwartzkroin, 1988) where incoming glutamatergic signals are summated and contribute substantively to the induction of learning-related LTP (Elfant et al, 2008; Pouille and Scanziani, 2001; 2004; Tukker et al, 2007). Interestingly, LTP itself can cause a progressive loss of I_A channel density in hippocampal CA1 pyramidal neurons (Jung and Hoffman, 2009). In addition, a decrease in I_A and I_A density after CIE in adolescence could relate to the well-known negative effects that chronic ethanol has on memory and hippocampal synaptic plasticity (see Monti et al, 1995).

Along with a decrease in the peak amplitude of I_A, CIE also produced a shift in the voltages at which I_A inactivation occurred. That is, after CIE, inactivation occurred at more

depolarized potentials in cells from CIE pretreated animals compared to those from their age-matched controls, but the age at which the CIE occurred did not influence the effect. This shift to the right of the I_A inactivation potential curves after CIE is an example of a way in which I_A is sensitive to CIE, but not developmentally so. It will be interesting to learn how interneurons with attenuated I_A functions after CIE will respond to acute ethanol challenge.

The functional consequences of diminished I_A in hippocampal interneurons after CIE may be quite broad. It has been shown that reductions in I_A function are associated with an increases in neuronal excitability. For example, attenuation of I_A has been associated with enhanced hyperexcitability in hippocampal pyramidal neurons following traumatic brain injury (Lei et al 2012). Moreover, the reduction of somatodendritic I_A channel function, or silencing Kv4.2 genes in hippocampal pyramidal cells, increases the generation of action potentials and burst firing (Kim et al 2005; Andrasfalvy et al 2008). The Kv4.3 subunits encoding I_A channels are distributed on somatodendritic compartments of CA1 interneurons exclusively (Bourdeau et al 2007, Menegola et al, 2008). By modulating these channels, especially those in the dendritic trees, the back-propagation of action potentials could be facilitated (Hoffman et al 1997; Migliore et al, 1999; Pan and Colbert, 2001). Furthermore, we have previously shown that ethanol increases the spontaneous firing rate of SLM interneurons (Yan et al, 2009) and that SLM interneurons from rats pretreated with CIE during adolescence tend to fire more in response to depolarizing current injections (unpublished observation). Thus, the long-term decrease in I_A activation after CIE during adolescence that we report here could represent a novel cellular mechanism to account for both the effects of CIE during adolescence on later memory function and the susceptibility of memory to disruption by acute ethanol.

Acknowledgments

This work was supported by National Institute of Alcoholism and Alcohol Abuse grant #U01-AA019925 (NADIA) to HSS, VA Career Development Award 2-010-10S to RLF, VA Career Development Award I01BX007080 to SKA, and a VA Senior Research Career Scientist awards to HSS and RAM from the Biomedical Laboratory Research and Development Service of the Department of Veterans Affairs Office of Research and Development.

References

Alekseev SI, Alekseev AS, Ziskin MC. Effects of Alcohols on A-Type K^+ Currents in Lymnaea Neurons. JEPT. 1997; 281:84–92.

An WF, Bowlby MR, Betty M, Cao J, Ling HP, Mendoza G, Hinson JW, Mattsson KI, Strassle BW, Trimmer JS, Rhodes KJ. Modulation of A-type potassium channels by a family of calcium sensors. Nature. 2000; 403:553–556. [PubMed: 10676964]

Andrásfalvy K, Makara JK, Johnston D, Magee JC. Altered synaptic and non-synaptic properties of CA1 pyramidal neurons in Kv4.2 knockout mice. J Physiol. 2008; 586:3881–3892. [PubMed: 18566000]

Binbaum SG, Varga AW, Yuan LL, Anderson AE, Sweatt JD, Schrader LA. Structure and function of Kv4-family transient potassium channels. Physiol Rev. 2004; 84:803–833. [PubMed: 15269337]

Bourdeau ML, Morin F, Laurent CE, Azzi M, Lacaille JC. Kv43-mediated A-type K+ currents underlie rhythmic activity in hippocampal interneurons. J Neurosci. 2007; 27:1942–1953. [PubMed: 17314290]

Bourdeau ML, Laplante I, Laurent CE, Lacaille JC. KChIP1 modulation of Kv4.30mediated A-type K $^{+}$ currents and repetitive firing in hippocampal interneurons. Neuroscience. 2011; 176:173–187. [PubMed: 21129448]

Cai SQ, Li WC, Sesti F. Multiple modes of A-type potassium current regulation. Current Pharmaceutical Design. 2007; 13:3178–3184. [PubMed: 18045167]

Carrasquillo Y, Burkhalter A, Nerbonne JM. A-type K+ channels encoded by Kv4.2, Kv4.3 and Kv1.4 differentially regulate intrinsic excitability of cortical pyramidal neurons. J Physiol. 2012; 590:3877–3890. [PubMed: 22615428]

Coetzee WA, Amarillo Y, Chiu J, Chow A, Lau D, McCormack T, Moreno H, Nadal MS, Ozaita A, Pountney D, Saganich M, Vega-Saenz de Miera E, Rudy B. Molecular diversity of K channels. Ann NY Acad Sci. 1999; 868:233–285. [PubMed: 10414301]

Cooper EC, Milroy A, Jan YN, Jan LY, Lowenstein DH. Presynaptic localization of Kv1.4-containing A-type potassium channels near excitatory synapses in the hippocampus. J. Neurosci. 1998; 18:965–997. [PubMed: 9437018]

Dahl RE. Adolescent brain development: a period of vulnerabilities and opportunities. Keynote address. Ann N Y Acad Sci. 2004; 1021:1–22. [PubMed: 15251869]

Elfant D, Zoltan B, Emptage N, Capogna N. Specific inhibitory synapses shift the balance from feedforward to feedback inhibition of hippocampal CA1 pyramidal cells. Eur J. Pharmacol. 2008; 27:104–113.

Empson RM, Heinemann U. The perforant path projection to hippocampal area CA1 in the rat hippocampal-entorhinal cortex combined slice. J. Physiol (Lond). 1995; 484:707–729. [PubMed: 7623286]

Freund TF, Buzsaki G. Interneurons of the hippocampus. Hippocampus. 1996; 6:347–470. [PubMed: 8915675]

Freund TF, Gulyas AI. Inhibitory control of GABAergic interneurons in the hippocampus. Can J Physiol Pharmacol. 1997; 75:479–487. [PubMed: 9250381]

Gonzalez LP. Electrophysiological changes after repeated alcohol withdrawal. Alcohol Health Res World. 1998; 22:34–37. [PubMed: 15706730]

Hoffman DA, Magee JC, Colbert CM, Johnston D. K+ channel regulation of signal propagation in dendrites of hippocampal pyramidal neurons. Nature. 1997; 387:869–875. [PubMed: 9202119]

Jerng HH, Pfaffinger PJ, Covarrubias M. Molecular physiology and modulation of somatodendritic A-type potassium channels. Mol Cell Neurosci. 2004; 27:343–369. [PubMed: 15555915]

Johnston J, Forsythe ID, Kopp-Scheinpflug C. Going native: voltage-gated potassium channels controlling neuronal excitability. J Physiol. 2010; 588:3187–3200. [PubMed: 20519310]

Jung SC, Hoffman DA. Biphasic Somatic A-Type K^{+} Channel Downregulation Mediates Intrinsic Plasticity in Hippocampal CA1 Pyramidal Neurons. PLoS One. 2009; 4:e6549. [PubMed: 19662093]

Jung SC, Kim J, Hoffman DA. Rapid, bidirectional remodeling of synaptic NMDA receptor subunit composition by A-type K+ channel activity in hippocampal CA1 pyramidal neurons. Neuron. 2008; 60:657–671. [PubMed: 19038222]

Kang J, Huguenard JR, Prince DA. Voltage-gated potassium channels activated during action potentials in layer V neocortical pyramidal neurons. J Neurophysiol. 2000; 83:70–80. [PubMed: 10634854]

Kim J, Hoffman DA. Potassium channels: Newly found players in synaptic plasticity. The Neuroscientist. 2008; 14:276–286. [PubMed: 18413784]

Kim J, Wei DS, Hoffman DA. Kv4 potassium channel subunits control action potential repolarization and frequency-dependent broadening in rat hippocampal CA1 pyramidal neurons. J Physiol (Lond). 2005; 15569:41–57. [PubMed: 16141270]

Khaliq ZM, Bean BP. Dynamic, nonlinear feedback regulation of slow pacemaking by A-type potassium current in ventral tegmental area neurons. J Neurosci. 2008; 28:10905–10917. [PubMed: 18945898]

Kole MHP, Letzkus JJ, Stuart GJ. Axon initial segment Kv1 channels control axonal action potential waveform and synaptic efficacy. Neuron. 2007; 55:633–647. [PubMed: 17698015]

Lacaille JC, Schwartzkroin PA. Stratum lacunosum-moleculare interneurons of hippocampal CA1 region. I. Intracellular response characteristics, synaptic responses, and morphology. J Neurosci. 1988; 8:1400–1410. [PubMed: 3357023]

Lei Z, Deng P, Li J, Xu ZC. Alterations of A-type potassium channels in hippocampal neurons after traumatic brain injury. J Neurotrauma. 2012; 20:235–245. [PubMed: 21895522]

Lien CC, Jonas P. Kv3 potassium conductance is necessary and kinetically optimized for high-frequency action potential generation in hippocampal interneurons. J Neurosci. 2003; 23:2058–2068. [PubMed: 12657664]

Lien CC, Martina M, Schultz JH, Ehmke H, Jonas P. Gating, modulation and subunit composition of voltage-gated K^+ channels in dendritic inhibitory interneurons of rat hippocampus. J Physiol (Lond). 2002; 538:405–419. [PubMed: 11790809]

Liss B, Franz O, Sewing S, Bruns R, Neuhoff H, Roeper J. Tuning pacemaker frequency of individual dopaminergic neurons by Kv4.3L and KChip3.1 transcription. EMBO J. 2001; 20:5715–5724. [PubMed: 11598014]

Littleton J. Neurochemical mechanisms underlying alcohol withdrawal. Alcohol Health Res World. 1998; 22:13–24. [PubMed: 15706728]

Lugo JN, Brewster AL, Spencer CM, Anderson AE. Kv4.2 knockout mice have hippocampal-dependent learning and memory deficits. Learning and memory. 2012; 19:182–189. [PubMed: 22505720]

Maffie J, Rudy B. Weighing the evidence for a ternary protein complex mediating A-type K^+ currents in neurons. J Physiol: (Lond). 2008; 586:5609–5623. [PubMed: 18845608]

Markwiese BJ, Acheson SK, Levin ED, Wilson WA, Swartzwelder HS. Differential effects of ethanol on memory in adolescent and adult rats. Alcohol Clin Exp Res. 1998; 22:416–421. [PubMed: 9581648]

Martina M, Schultz JH, Ehmke H, Monyer H, Jonas P. Functional and molecular differences between voltage-gated K+ channels of fast-spiking interneurons and pyramidal neurons of rat hippocampus. J Neurosci. 1998; 18:8111–8125. [PubMed: 9763458]

Marty VN, Spigelman I. Long-lasting alterations in membrane properties, k(+) currents, and glutamatergic synaptic currents of nucleus accumbens medium spiny neurons in a rat model of alcohol dependence. Front Neuroscience. 2012; 6:3–15.

Menegola M, Hisonou H, Vacher H, Trimmer JS. Dendritic A-type potassium channels subunit expression in CA1 hippocampal interneurons. Neuroscience. 2008; 154:953–964. [PubMed: 18495361]

Migliore M, Hoffman DA, Magee JC, Johnston D. Role of an A-type K+ conductance in the back-propagation of action potentials in the dendrites of hippocampal pyramidal neurons. J Comput Neurosci. 1999; 7:5–15. [PubMed: 10481998]

Monti PM, Miranda R, Jr. Nixon K, Sher KJ, Swartzwelder HS, Tapert SF, White A, Crews FT. Adolescence: booze, brains, and behavior. Alcohol Clin Exp Res. 2005; 29:207–220. [PubMed: 15714044]

Morin F, Haufler D, Skinner FK, Lacaille JC. Characterization of voltage-gated K^+ currents contributing to subthreshold membrane potential oscillations in hippocampal CA1 interneurons. J Neurophysiol. 2010; 103:3472–3489. [PubMed: 20393060]

NIAAA. 10th Special Report to the U.S. Congress on Alcohol and Health. US Deparment of Health and Human Services; 2000.

Pan EH, Colbert CM. Subthreshold Inactivation of Na^+ and K^+ Channels Supports Activity-Dependent Enhancement of Back-Propagating Action Potentials in Hippocampal CA1. J Neurophysiol. 2001; 85:1013–1016. [PubMed: 11160533]

Pouille F, Scanziani M. Enforcement of temporal fidelity in pyramidal cells by somatic feed-forward inhibition. Science. 2001; 293:1159–1163. [PubMed: 11498596]

Pouille F, Scanziani M. Routing of spike series by dynamic circuits in the hippocampus. Nature. 2004; 429:717–723. [PubMed: 15170216]

Sircar R, Sircar D. Adolescent rats exposed to repeated ethanol treatment show lingering behavioral impairments. Alcohol Clin Exp Res. 2005; 29:1402–1410. [PubMed: 16131847]

Swartzwelder HS, Wilson WA, Tayyeb MI. Age-dependent inhibition of long-term potentiation by ethanol in immature versus mature hippocampus. Alcohol Clin Exp Res. 1995; 19:1480–1485. [PubMed: 8749814]

Tavian D, De Giorgio A, Granato A. Selective underexpression of Kv3.2 and Kv3.4 channels in the cortex of rats exposed to ethanol during early postnatal life. Neurol Sci. 2011; 32:571–577. [PubMed: 21234782]

Tkatch T, Baranauskas G, Surmeirt DJ. Kv4.2 mRNA abundance and A-type K^+ currents amplitude are linearly related in basal ganglia and basal forebrain neurons. J Neurosci. 2000; 20:579–588. [PubMed: 10632587]

Treistman SN, Wilson AH. Effects of ethanol on early potassium currents in Aplysia: Cell-specificity and influence of channel state. Journal of Neuroscience. 1987; 7:3207–3214. [PubMed: 2444677]

Tukker J, Fuentealba P, Hartwich K, Somoguyi P, Klausberger T. Cell Type-Specific Tuning of Hippocampal Interneuron Firing during Gamma Oscillations In Vivo. J. Neurosci. 2007; 27:8184–8189. [PubMed: 17670965]

Vida I, Halasy K, Szinyei C, Somogyi P, Buhl EH. Unitary IPSPs evoked by interneurons at the stratum radiatum-stratum lacunosum-moleculare border in the CA1 area of the rat hippocampus in vitro. J Physiol (Lond). 1998; 506:755–773. [PubMed: 9503336]

White AM, Ghia AJ, Levin ED, Swartzwelder HS. Binge pattern ethanol exposure: differential impact on subsequent responsiveness to ethanol. Alcohol Clin. Exp. Res. 2000; 24:1251–1256. [PubMed: 10968665]

Yan HD, Li Q, Fleming R, Madison R, Wilson W, Swartzwelder HS. Developmental Sensitivity of Hippocampal Interneurons to Ethanol: Involvement of the Hyperpolarization-Activated Current. Ih. J Neurophysiol. 2009; 101:67 – 83.

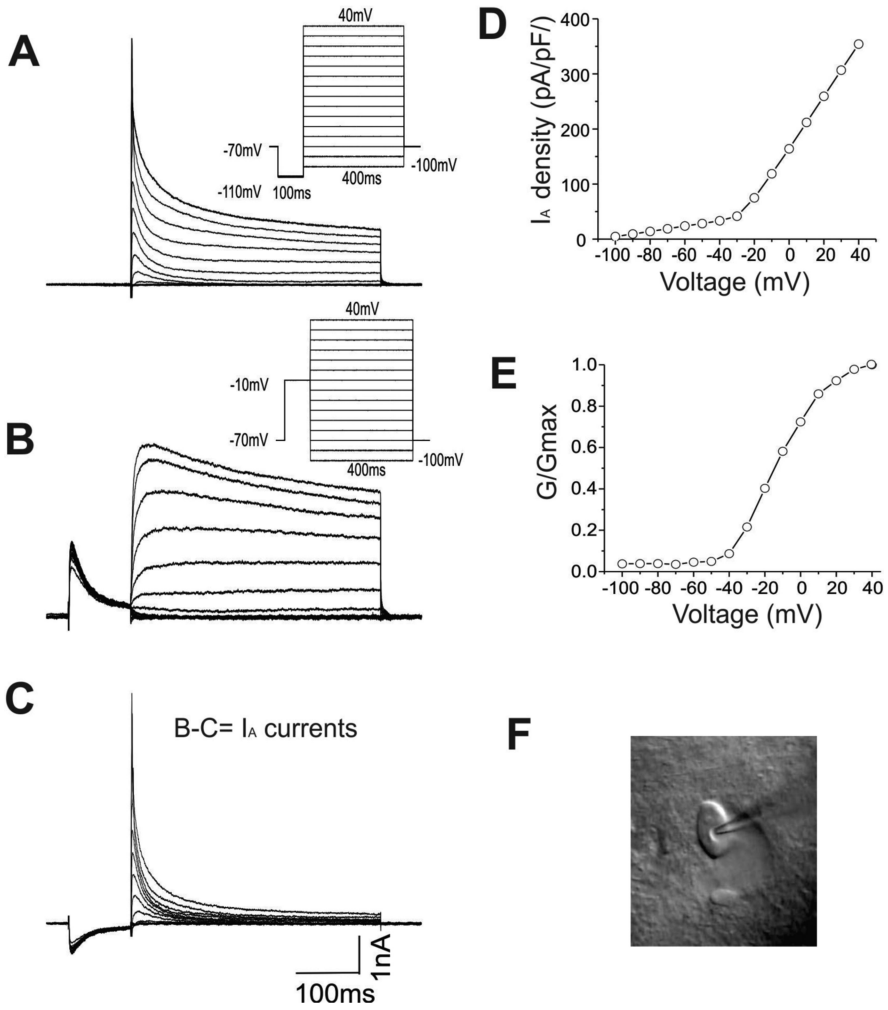

Figure-1. Isolation of I_A currents in CA1 interneurons

A: A whole-cell voltage-clamp recording of the outward currents evoked by a series of depolarizing voltage steps from -100 mV to + 40 mV following a hyperpolarizing step to -110 mV from a holding potential of -70 mV to enable the maximal I_A conductances. Inset: voltage protocols.

B: Outward currents elicited by the same protocol with a prepulse of -10 mV to inactivate I_A channels. Inset: voltage protocols.

C: The fast activating and inactivating I_A currents were isolated by digitally subtracting the currents from panel C from those in panel B.

D. The voltage dependence of the normalized I_A conductance in the same interneuron.

E. Photomicrograph of an interneuron located in SR sub-region of the hippocampus is shown.

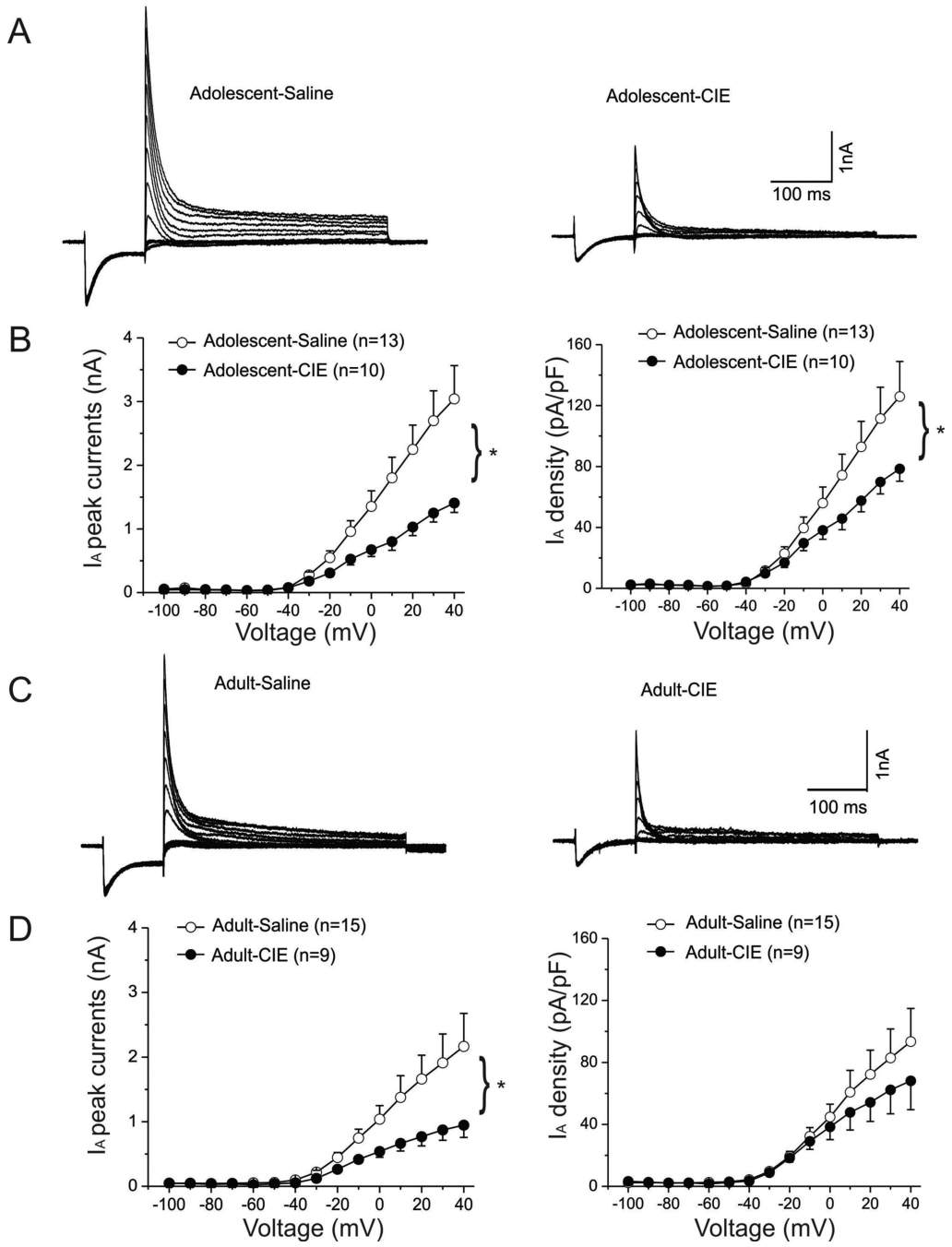

Figure-2. Suppression of I_A peak currents in interneurons from rats that had been previously treated with CIE during adolescence or adulthood

A. Representative I_A currents traces elicited by depolarizing voltage steps are shown for interneurons from an adolescent-saline (left panel) and an adolescent-CIE rat (right panel).

B. CIE treatment significantly reduced the mean I_A peak currents when interneurons were depolarized above -20 mV (left panel * $p<0.05$). Changes in I_A current densities are shown in the right panel and were also significantly suppressed (* $p<0.05$).

C. Representative I_A current traces elicited by depolarizing voltage steps are shown for interneurons from an adult-saline (left panel) and an adult-CIE rat (right panel)

D. CIE treatment significantly reduced the mean I_A peak currents after interneurons were depolarized above -20 mV (left panel, * $p<0.05$). Changes in I_A current densities are shown in the right panel.

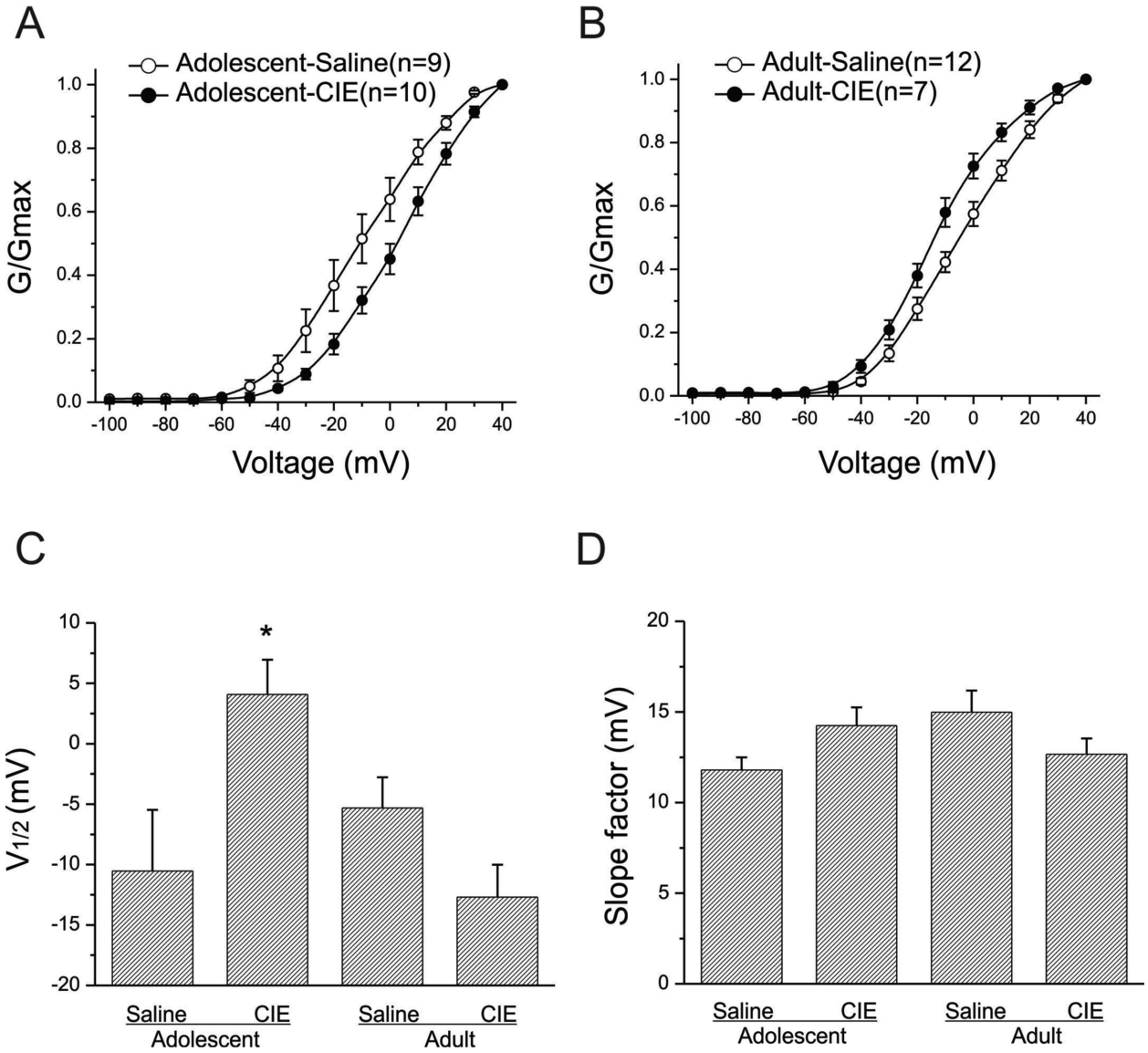

Figure-3. Steady-state activation of I_A channels in interneurons from both adolescent-CIE and adult-CIE rats

A: Steady-state activation curves of I_A channels of interneurons from adolescent-saline and adolescent-CIE rats are shown.

B: Steady-state activation curves of I_A channels of interneurons from adult-saline and adult-CIE rats are shown.

C: Bar graphs illustrating the mean half-activation potentials of I_A currents for adolescent and adult rats. Interneurons from rats that had been treated with CIE during adolescence had a significantly more depolarized half-activation potential than did those from rats treated with saline during adolescence(*$p<0.05$). However, there was no significant difference in the in the half activation potential in interneurons from rats treated during adulthood with saline or CIE ($p>0.05$).

D: Bar graphs illustrating the mean slope factors of steady-state activation of I_A currents for adolescent and adult rats. Pretreatment with ethanol during adolescence or adulthood did not alter the slope factors of I_A activation ($p>0.05$).

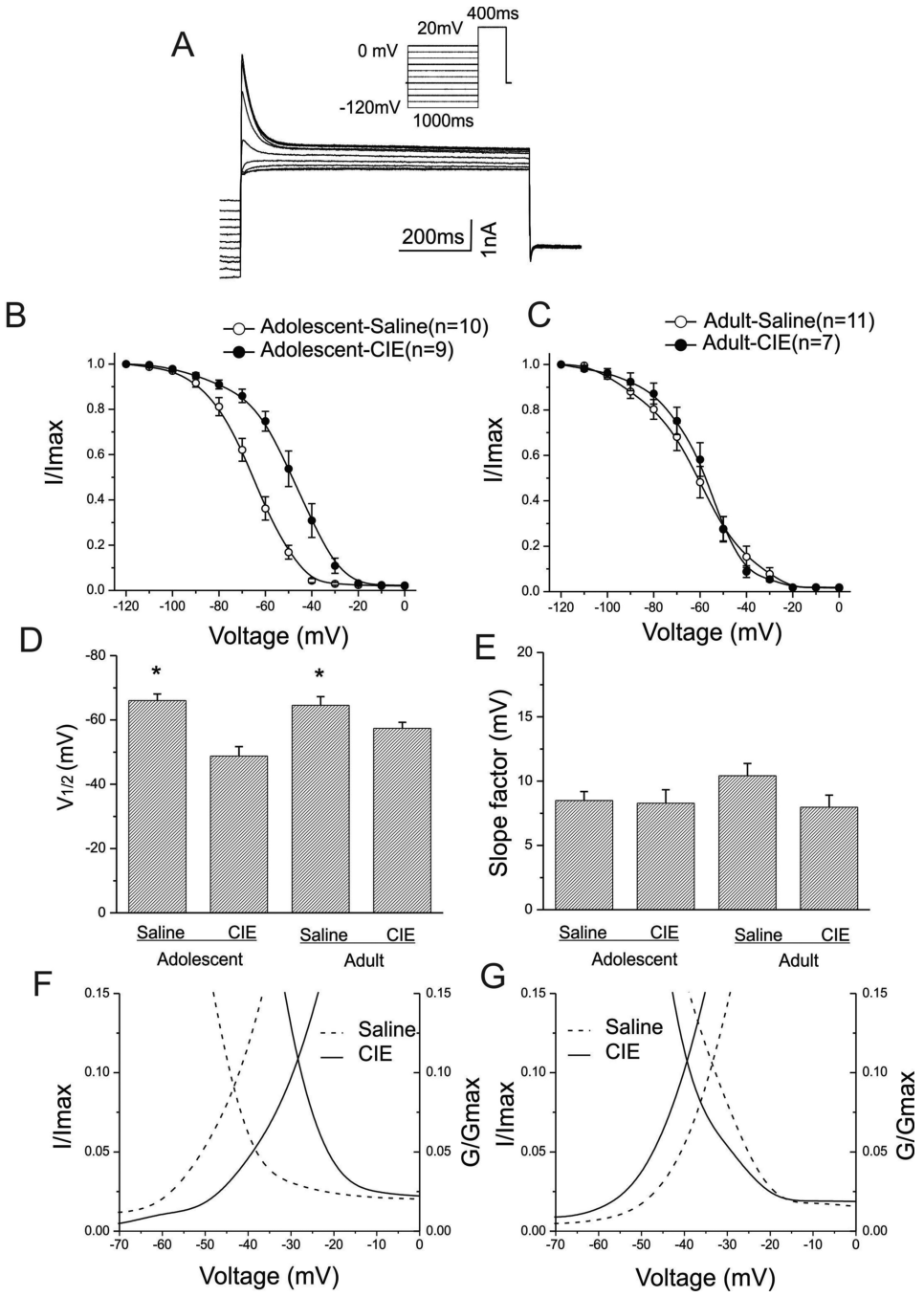

Figure-4. Steady-state inactivation of I_A currents in interneurons from both adolescent-CIE and adult-CIE rats

A: Representative I_A current traces elicited by depolarizing voltage steps are shown for an interneuron. Inset: voltage protocols

B: Steady-state inactivation curves of I_A currents of interneurons from adolescent-saline and adolescent-CIE rats are shown.

C: Steady-state inactivation curves of I_A currents of interneurons from adult-saline and adult-CIE rats are shown.

D: Bar graphs illustrating the mean half-inactivation potentials of I_A currents for adolescent and adult rats. Adolescent-CIE rats had a significantly more depolarized half inactivation potential than that of adolescent-saline rats (*$p<0.05$). Similarly, there was a significant difference in the half inactivation potentials between adult saline and CIE rats (*$p<0.05$).
E: Bar graphs illustrating the mean slope factors of steady-state inactivation of I_A currents for adolescent and adult rats. There were no significant differences in the mean slope factors among these groups ($p>0.05$).
F: Intersection of average activation and inactivation curves of I_A in interneurons from adolescent rats pretreated with either saline (dotted lines) or ethanol (solid lines) are shown. The areas under intersections represent a window current. CIE exposure shifts the intersection to the right when compared to that in saline group.
G. Intersection of average activation and inactivation curves of I_A in interneurons from adult rats pretreated with either saline (dotted lines) or ethanol (solid lines) are shown. The areas under intersections represent a window current. CIE exposure shifts the intersection slightly to the left compared to that in saline group.

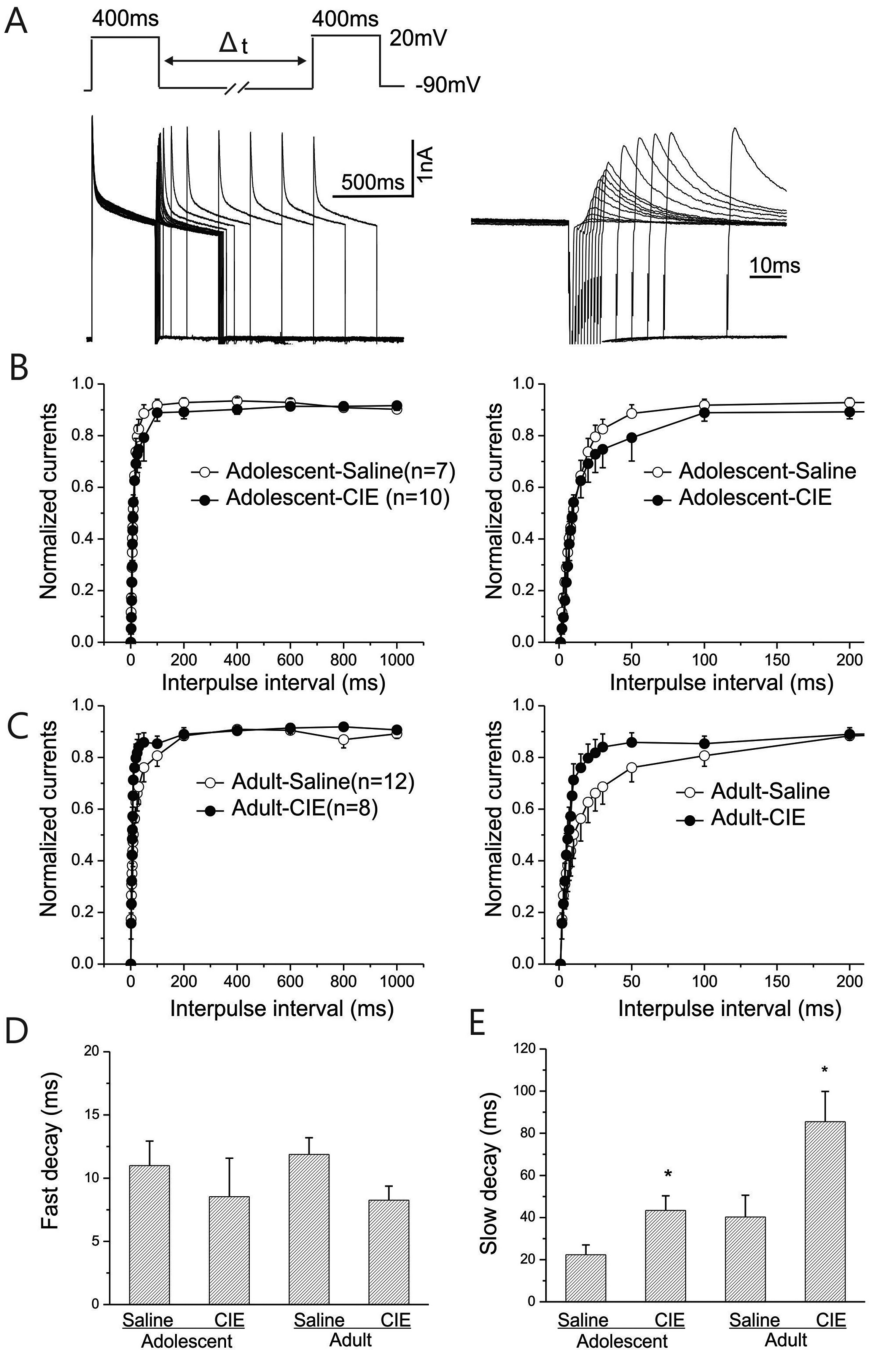

Figure-5. Dynamic changes in the recovery from inactivation of I_A currents in interneurons from adolescent-CIE and adult-CIE rats

A: Left panel: Representative current responses recorded for determining recovery from inactivation of I_A currents from an interneuron are shown. A progressive increase in the Amplitude of outward peak currents was evoked by paired pulses to +40 mV for 400 ms starting from a conditioning step of-90 mV with a variable interpulse interval (Δt) ranging between 1 and 1000 ms. Right panel: enlargement of the same responses is shown for the first 200 ms.

B: Mean normalized peak currents are plotted as a function of recovery time (left panel), and the enlargement of the first 200 ms of the plot (right panel) is shown for adolescent saline and CIE-rats.

C: Mean normalized peak currents are plotted as a function of recovery time (left panel), and the enlargement of the first 200 ms of the plot (right panel) is shown for adult-saline and adult– CIE rats.

D: The time course of the recovery for each interneuron from inactivation of I_A was fitted with a double exponential function. Fast decay times for adolescent and adult rats are shown for comparison. The mean fast decay time constants for the adolescent- and adult-CIE rats were slightly faster than that of the rats treated with saline, but the difference was not statistically significant ($p>0.05$).

E: The slow decay time constants of the recovery from inactivation of I_A for adolescent and adult rats are shown. The time courses of the slow decay for the adolescent- and adult-CIE rats were slower than that of the rats treated with saline (*$p <0.05$).

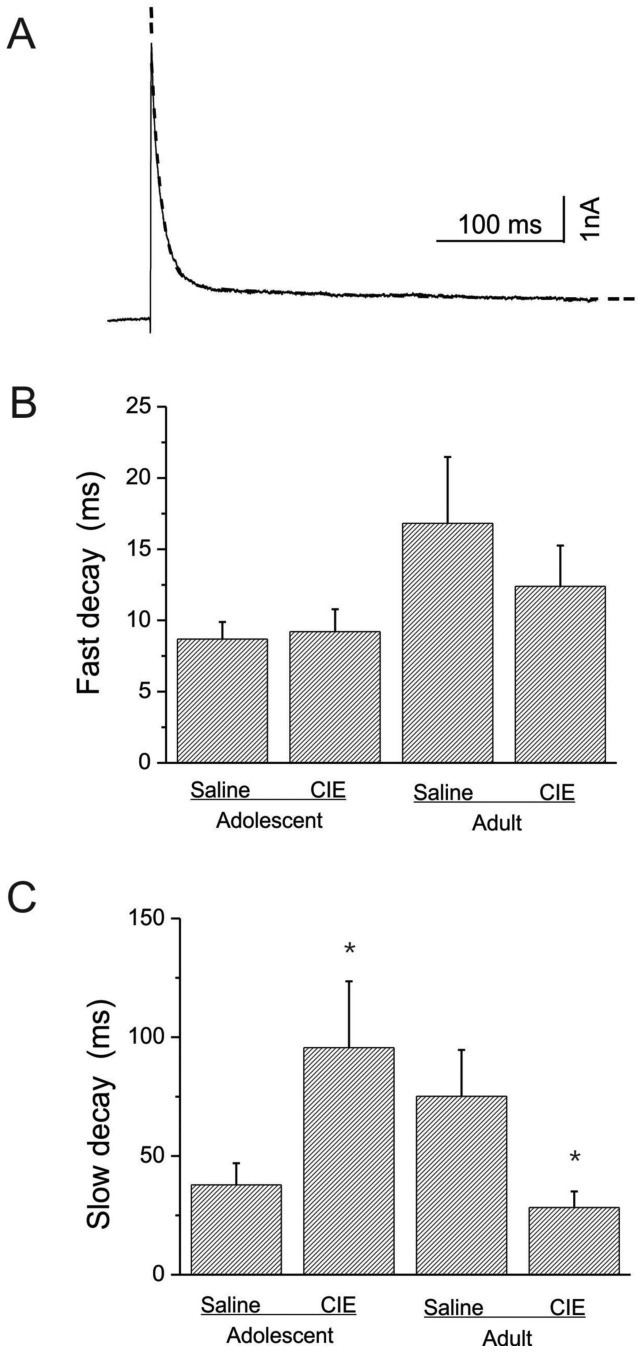

Figure-6. The decay kinetics of I_A peak currents in interneurons from adolescent-CIE and adult-CIE rats

A: A representative example of averaged I_A current traces elicited by depolarization to +30 mV was fitted by double exponential function (dotted line).

B: Bar graphs illustrating the mean fast decay time constants for adolescent-saline (n=13), adolescent-CIE (n=12) and adult-saline (n=15) and -CIE (n=9) rats. No statistical difference in the mean fast time constants between adolescent-saline and -CIE rats or between adult-saline and –CIE rats were detected ($p>0.05$).

C: bar graphs illustrating the slow decay time constants for adolescent-saline (n=13), adolescent-CIE (n=12) and adult-saline (n=15) and -CIE (n=9) rats. Adolescent-CIE rats showed a significantly slower decay time constants than that of the age-matched controls (*$p<0.05$). Adults-CIE rats showed a significantly fast decay time constants than that of the age-matched controls (*$p<0.05$)